ICAS 2016
30th Congress of the International Council of the Aeronautical Sciences
DCC, Daejeon, Korea ; September 25-30, 2016

MISSION BASED COMPARISON OF SINGLE- AND COUNTER-ROTATING FAN DESIGNS

Tom Otten, Timea Lengyel-Kampmann
German Aerospace Center, Institute of Propulsion Technology

Keywords: *Counter Rotating Fan, Engine concepts*

Abstract

Aircraft fuel efficiency becomes more and more important because of increasing fuel prices and environmental concerns. Engine efficiency contributes substantially to this, but further improvements are very demanding due to the already mature technology. To achieve further enhancements, the introduction of new engine concepts is currently in discussion. In this context, the German Aerospace Center is currently investigating the potential of a counter rotating fan.
The aim of this study is to determine the quantitative efficiency difference between a counter rotating fan and a conventional high bypass ratio (geared) fan. This study includes aerodynamical and mechanical design studies as well as overall engine performance simulations. Besides efficiency differences, the effects of weight and size are taken into account and the fuel consumption on a flight mission is calculated and compared for both concepts.

0 Nomenclature

AN^2	Blade Loading Parameter
BPR	Bypass Ratio
CR-fan	Counter Rotating Fan
c_u	Circumferential Velocity
EoF	End of Field
h	Enthalpy
HPC	High Pressure Compressor
HP-shaft	High Pressure Shaft
HPT	High Pressure Turbine
L/D	Lift-to-Drag Ratio
LPC	Low Pressure Compressor
LP-shaft	Low Pressure Shaft
LPT	Low Pressure Turbine
m	Mass
$Ma_{ax,fan}$	Axial Fan Inlet Mach Number
OPR	Overall Pressure Ratio
PDG	Planetary Differential Gear
R	Range
SR-fan	Single Rotating Fan
TET	Turbine Entry Temperature
TOC	Top of Climb
TSFC	Thrust Specific Fuel Consumption
v	Flight Speed
η_{prop}	Propulsive Efficiency
Π_{fan}	Fan Pressure Ratio
Ψ	Work Coefficient
Δ	Difference

Subscripts:

ax	Axial
cont	Containment
corr	Corrected
CR	Counter Rotating
is	Isentropic
L	Landing
mod	Modified
rel	Relative
SR	Single Rotating
t	Total
0	Before fan
2	After fan

1 General Introduction

Counter rotating fans (CR-fans) provide a promising possibility to improve the overall efficiency of today's aero engines. By splitting the total pressure rise into two stages, low blade numbers per row and high axial Mach numbers can be achieved. This in turn leads to lower fan diameters compared to direct driven or geared turbofans assuming an equal bypass ratio (BPR). As the second rotor removes most of the swirl induced by the first stage, no stator is

required for this concept. The absence of stator losses combined with low stage loadings enable very high fan efficiencies, high bypass ratios and high propulsive efficiencies.

The planetary differential gear (PDG) was found to be the most suitable solution to drive both fan stages with only one high-speed power turbine.

It has been shown, that the introduction of a PDG creates new limitations for aerodynamic design, resulting in non-axial flow after the second rotor that reduces the propulsive efficiency [1]. As the PDG is a torque splitting device, the arising dependency between rotor speed ratios and power ratios must be considered at part load conditions. These intrinsic characteristics of the PDG have an effect on fan performance and must be accounted for in engine performance calculations as well as aerodynamic simulations.

Several studies [2][3][4] already dealt with the aerodynamic optimization of CR-fans for specific axial Mach number and total pressure ratio combinations, covering the entire range from current to potential future ultra-high bypass ratio engines. The results of these studies showed an isentropic efficiency benefit of the CR-fan compared to the conventional single-rotating fan (SR-fan), which strongly depends on the selected applications. Following this experience, the influence of the fan total pressure ratio and fan inlet axial Mach number on the efficiency benefit was determined more precisely through a generalized 3D-optimization with a RANS-Solver [5].

To evaluate the effects of the axial fan inlet Mach number and the fan pressure ratio, it is important to consider not only the efficiencies but also the fan weight. Furthermore, the fan design has influence on the overall engine design since the selection of an axial fan Mach number is a compromise of fan weight and drag (which are best at high axial Mach numbers) and fan efficiency (which is best at low axial Mach numbers). Hence, the selection of the best fan pressure ratio is basically a trade-off between propulsive efficiency, drag and weight.

To assess the results of the aerodynamic optimization on a more global level, a weight estimation of the fan module was added to the aerodynamical optimization, and a mission based cycle design study was performed to evaluate the CR-fan module on engine level to identify the best aerodynamic design of the counter rotating fan [6][7].

This study is divided into two fields of activity:

First, a multidisciplinary optimization is carried out to maximize isentropic efficiency and to minimize the weight of the fan module. The optimization is performed independently for the counter-rotating and for the single-rotating fan concepts. To ensure comparable results, the same process chain, the same parametrization and the same restrictions are applied.

These results are then transferred to a mission based cycle design study as response surfaces. For a civil long range application, the aircraft characteristics are modelled and engine requirements are derived. Then a cycle is developed for each point on the response surfaces, taking all constraints from the aircraft as well as several thermodynamic limitations into account.

As a result the best aerodynamic fan design for each concept is identified by finding the best compromise between cycle demands, fan efficiency, weight and drag in order to minimize the overall fuel consumption.

Finally, the potential of the gear driven counter rotating fan concept is discussed and compared to more conventional single rotating fans.

2 Aerodynamic optimization

2.1 Methods

The target of the aerodynamic optimization is to determine the correlation between optimized fan weight and modified efficiency as a function of the fan inlet axial Mach number $Ma_{ax,fan}$ and fan pressure ratio Π_{fan} for both counter-rotating and single-rotating fan concepts.

The modified fan efficiency (η_{mod}) is calculated by Eq. 1, in which the kinetic energy of the exit swirl is considered as an additional loss in the isentropic efficiency term [1].

$$\eta_{mod} = \frac{h_{2t,is} - h_{0t} - \frac{c_u^2}{2}}{h_{2t} - h_{0t}} \qquad (1)$$

In the following, the values for η_{mod} are shown as the difference to a constant reference value.

The fan weight includes the weight of all fan rotor and stator blades, the related discs and the fan containment (Eq. 2) [6].

$$m_{Fan} = m_{Blades} + m_{Disc} + m_{Cont} \qquad (2)$$

In [6], the detailed optimization approach was already discussed and applied to the CR-fan at a narrow fan pressure range $\Pi_{fan} \in [1.3\text{-}1.35]$. Figure 1 shows the achieved correlation between modified efficiency and fan module weight at different axial inlet Mach numbers. Since $Ma_{ax,fan}$ is defined as an equally distributed parameter ([5],[6]) in the optimization with a step size of 0.025, the whole examined $Ma_{ax,fan}$ range [0.6-0.75] can be covered in one optimization process. This results in one specific Pareto-front for each $Ma_{ax,fan}$ interval.

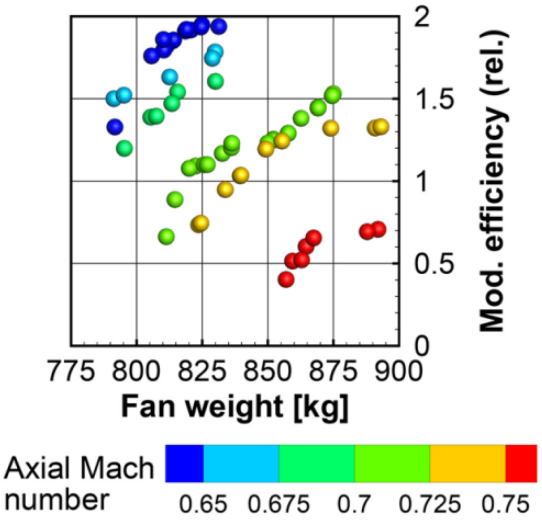

Figure 1: Optimization results of the CR-fan for 1.3< Π_{fan}<1.35. Modified efficiency is shown as difference to reference value in %-points.

In this paper, this optimization process is carried out for 4 different fan pressure ratio ranges (Π_{fan} = [1.25-1.3]; [1.3-1.35]; [1.35-1.4]; [1.4-1.45], see Figure 2) and applied to both the SR- and CR-fan concept.

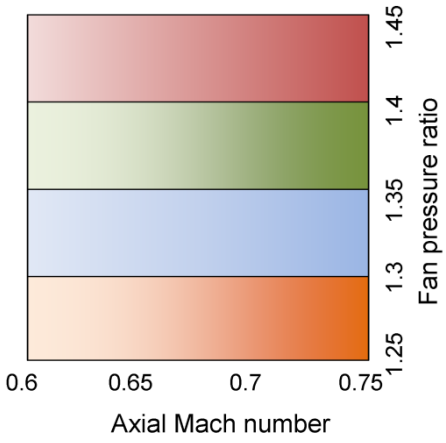

Figure 2: The examined fan pressure ratio – axial inlet Mach number range

2.2 The optimization process chain

The optimization process chain can be divided into an aerodynamic and a mechanic part (Figure 3).

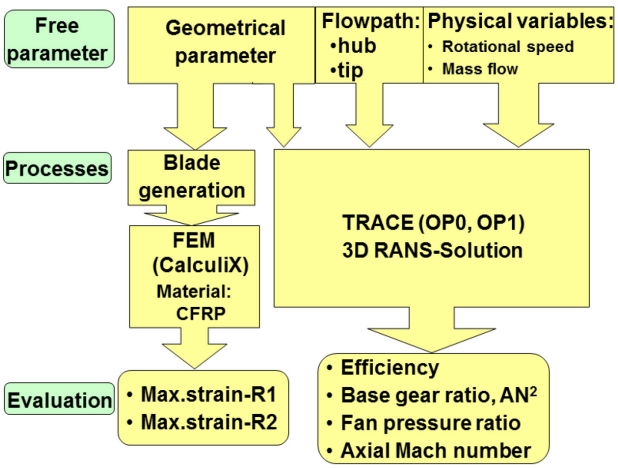

Figure 3: Process chain of the 3D RANS + FEM optimization

The aerodynamic process starts with the generation of the flow path and the blades based on a 3D parametrization shown in [6]. Subsequently the meshing of the fluid volume and the definition of boundary conditions for the 3D CFD simulation are carried out. Finally the CFD simulation with the DLR in-house code TRACE [8] is performed in two operating points (Aerodynamical Design Point and a near-stall point). The automatic evaluation completes the aerodynamic process chain by calculating Π_{fan}, $Ma_{ax,fan}$ and modified efficiency among other data.

In case of the CR-fan, a limitation of the LP-shaft speed is required to avoid unrealistic gearbox designs [1]. In an engine performance pre-study, the maximum allowable LP-shaft speeds were defined as a function of fan pressure ratio and axial Mach number [6].

A structural analysis is carried out for the rotor blades by applying the non-commercial FEM solver CalculiX [9]. The rotor blades consist of 80% CFRP material and 20% titanium to reduce the fan module weight. The maximal strain of the rotor blades is restricted.

The final process is the determination of the fan module weight. The calculation of the blades weight is based on the volume and density. A correlation was generated in [6] to estimate the optimal disc weight as function of a few blade-dependent parameters. The containment weight is estimated by an empirical correlation [6].

2.3 Optimization results

The optimization process chain was carried out by means of the DLR in-house multiobjective automatic optimization code "Auto-Opti" ([4][5][10][11]), which is based on an evolutionary algorithm. The code is extended with a special add-on to use uniformly distributed parameters (EDSQ). Surrogate models (in this case Kriging) are used to accelerate the optimization process. The fitness functions in the optimizations were defined as follows:

- maximize the modified fan efficiency
- minimize the fan module weight

In each optimization, the fan pressure ratio was restricted to a small range (Π_{fan} = [1.25-1.3]; [1.3-1.35]; [1.35-1.4]; [1.4-1.45]). The lowest fan pressure ratio in each range proved to be the best compromise to reach better fitness values.

Figure 4 shows the Pareto-fronts of the CR-fan optimizations for the different fan pressure ratios (1.25; 1.3; 1.35 and 1.4) and different axial inlet Mach numbers. Figure 5 shows the corresponding results of the SR-fan optimizations.

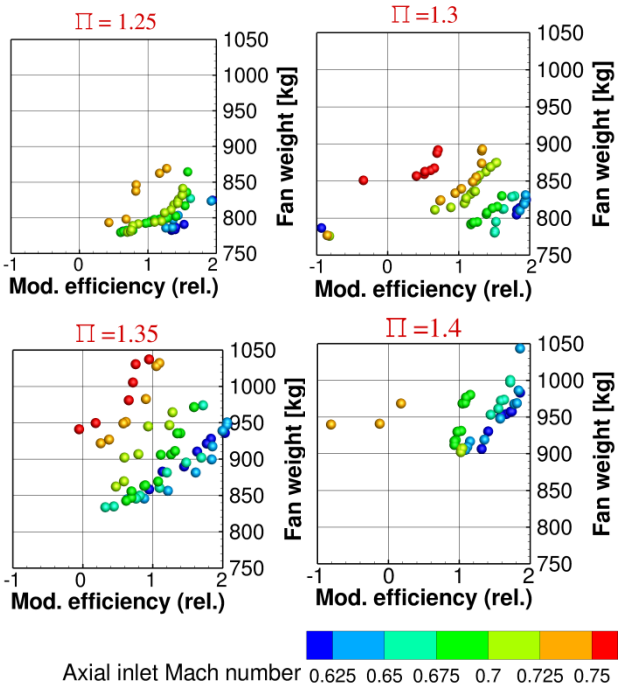

Figure 4: Pareto-fronts of the CR-fan optimizations with different fan pressure ratios

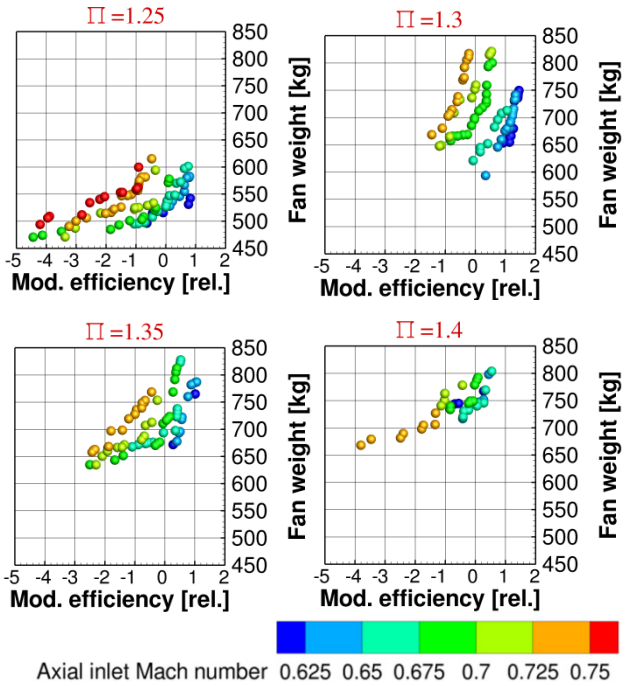

Figure 5: Pareto-fronts of the SR-fan optimizations with different fan pressure ratios

In comparison to the CR-fan results, the achieved fan weight of the SR concept decreases by about 150-200kg for the same fan diameter. This is referable to the additional disc

of the CR-fan for the second rotor. On the other hand the achieved efficiency is higher for the CR-fan. With higher axial inlet Mach numbers, the efficiency benefit of the CR-fan increases.

Figure 5 shows a broad Pareto-front range for the SR-fan optimizations. In this case the correlation between the efficiency and the fan weight is stronger than for the CR-fan.

The shape of the Pareto-fronts of the CR-fans is spire-shaped, which means the weight can be reduced without a significant loss in efficiency. The width of the Pareto-fronts is only about 1% in efficiency and 50-100 kg in weight.

These correlations will be applied in the following thermodynamic cycle evaluation to find a compromise between the fan weight and efficiency regarding the mission fuel burn.

2.4 Evaluation of the results

Each of the plots in Figure 4 and Figure 5 can be shown as a 3D surface with the three variables: axial inlet Mach number, fan weight and modified efficiency (Figure 6 and Figure 7).

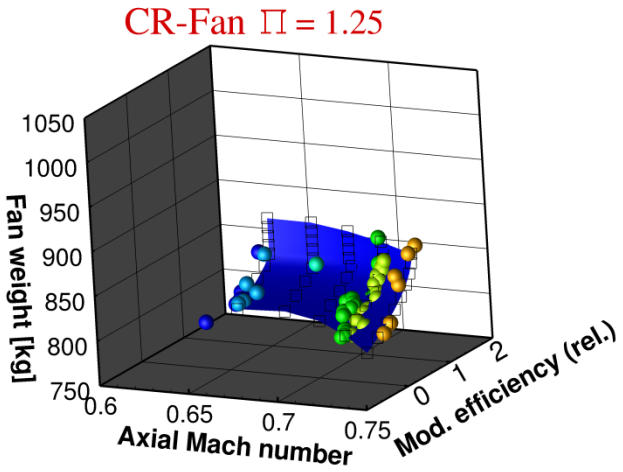

Figure 6: 3D-surface based on the Pareto-fronts of the CR fan optimization at Π_{FAN} =1.25

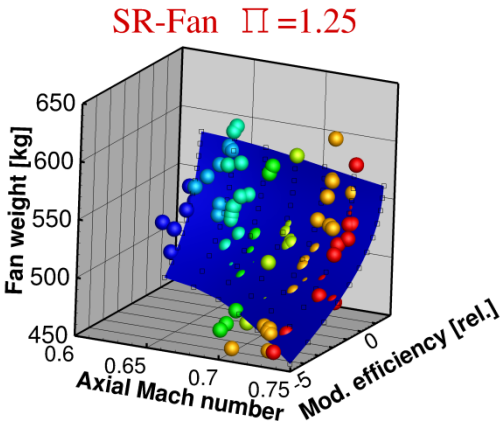

Figure 7: 3D-surface based on the Pareto-fronts of the SR-fan optimization at Π_{FAN} =1.25

Since the Pareto-fronts are never completely converged, a Kriging-approximation with a Quasi Newton minimizing method was applied to get a smooth surface [12]. These surfaces are defined through equally distributed data points on the axial inlet Mach number ($Ma_{ax,fan}$) – fan weight (m_{Fan}) plane. Thus the modified efficiency can be accessed as $\eta_{mod}=f(Ma_{ax,fan}, m_{Fan})$.

In the first step the Pareto-fronts of the optimizations with the different fan pressure ratios are merged to create the Kriging-model. This step allows using not only $Ma_{ax,fan}$ and m_{fan}, but also Π_{fan} as a variable in the Kriging model. This is necessary, because the fan pressure ratio was not the same for each member in one optimization, thus it was given as an interval. The merged Pareto-fronts provide information about the Π_{fan}-gradients as well.

In a second step surfaces for modified efficiency, rotor speed, exit flow angle and base gear ratio (for the CR-fan) were created with the following variables:

- fan pressure ratio
- axial inlet Mach number
- fan weight

These surfaces give the input for the engine cycle calculations in the following chapter for both the CR and the SR-fans.

3 Cycle Design

The comparison of the multiple aerodynamic fan designs requires the balancing of the fan

weight, its efficiency and its usability in future engine designs. As the fan design has a large effect on the engine design, an engine cycle design study is performed and the weight and drag of the overall engine is calculated. Then a flight mission analysis is conducted to calculate the mission fuel burn which is used as a figure of merit that includes the engine performance, its weight, drag and efficiency. A detailed presentation of the related methodology can be found in [7].

3.1 Methods

Engine performance calculation

The evaluation of the counter rotating and single rotating Fans on engine level was performed with DLR's in-house performance code GTlab-Performance [25]. In order to allow for a direct comparison of both fan concepts, a cycle was designed for discrete points on the Pareto fronts defined in chapter 2.

The engine setups for the SR and CR-fans are very similar and differ only in the fan section. All the engines are designed as two-shaft geared unmixed turbofans. The core engine components are modelled using standard component maps. The component modelling is based on [7]. The two stage high-pressure turbine (HPT) is cooled, while the low pressure turbine (LPT) is assumed to be uncooled. The influence of component size on efficiency is modelled according to [13]. The effect of cooling air on HPT efficiency is also included in the performance model [13].

By matching the nozzle speed ratio to the ideal nozzle speed ratio, the bypass ratio is defined [26]. The intake mass flow is adapted to match the thrust requirements. The pressure ratio split between HPC and LPC is assumed to be constant.

The rotational speed of the HP-shaft is defined by fixing the maximum tip speed of the HPC to 390m/s based on data presented in [13].

The main limitation for the LP-shaft speed results from the AN^2 at the exit of the LPT which describes the blade airfoil stress of the LPT. Here, the highest values are typically found at takeoff conditions and should not exceed 12400 m^2/s^2 [13]. In this study, the LP-shaft speed is a result of the assumed gearbox transmission ratio which is defined in the aerodynamic design. A performance pre-study was conducted to define maximum LP-shaft speeds for the aerodynamic design.

The LP-shaft speed of the SR-fan is not defined by the fan aerodynamics as the gearbox transmission ratio can be adapted without influencing the aerodynamic design. In this study, the LP-speed is defined by assuming the same LPT AN^2 as for the CR-fans.

In order to achieve best engine efficiency, a high overall pressure ratio (OPR) and turbine entry temperature (TET) are desirable. By limiting the highest off-design HPC exit temperature to 970K and the LPT entry temperature to 1250K, the design-OPR and TET are indirectly defined.

The cycle is designed for cruise condition, as this is the most important point in terms of fuel consumption, especially for a long range design. Relevant off-design points such as End of Field (EoF) and Top of Climb (TOC) are regarded in order to verify maximum thermal and mechanical loads.

In this study, the fan pressure ratio (Π_{fan}) is a free parameter. Especially for low Π_{fan}, a variable area bypass nozzle will become necessary to ensure save surge margins at critical off-design points like Take-off/EoF condition. The nozzle area is adapted to match a given distance from surge line in the fan performance map in order to ensure stable operation.

Fan and Gearbox modelling

Both fan concepts are assumed to be driven by a planetary gearbox. A constant mechanical efficiency of the gearbox is assumed.

The fans efficiencies are directly taken from the aerodynamic fan calculation.

The aerodynamic fan design was performed for a constant diameter. During engine performance calculations, the fan is scaled in size to match the thrust and cycle requirements.

For both the SR and the CR-fan, performance maps were calculated for representative aerodynamic designs and then scaled to the individual engine design point.

For the CR-fan, the performance map was calculated assuming a constant torque ratio between both fan stages as described in [1]. Besides the modified efficiency, the base gear ratio and the rotational speed ratio between both rotors are used to calculate the speed ratio between LPT and the rotors in the performance off-design calculation.

Engine weight estimation

The best engine setup is not solely defined by engine efficiency. The engine weight and drag contributes significantly to the efficiency of the overall aircraft system.

The determination of the total engine weight is inherently difficult in this stage of development, as only brief descriptions of its components are available.

Using thermodynamic cycle parameter together with estimates of Mach numbers and hub-to-tip ratios a preliminary annulus design can be derived.

Component	Work coefficient $\bar{\Psi} = \frac{\Delta h}{{c_u}^2}$
LPC	0.4
HPC	0.5
LPT	1.3

Table 1: Max. allowed stage loadings

By assuming maximum average stage loadings for LPC, HPC and LPT (Table 1, from [13], [15]), the number of stages is calculated. Hence, a bare engine flow path can be defined which provides the input parameters for the subsequent components weight and nacelle geometry calculations.

The fan weight for a reference fan diameter is directly taken from the aerodynamic design results. For the scaling to the actual fan size, the gradients of the weight correlation method presented in [16] are applied.

The gearbox weight is correlated using the methodology presented in [20]; the results correspond very well to the data presented in [13].

The weight of the other engine components is modelled according to [16]. The component weights derived by this method are corrected to match internal reference data as well as public available engine weights [18]. The determination of the engine nacelle weight is performed by a simple correlation developed in [19].

The drag of the engine nacelle is determined by means of the component build up methodology proposed by [21]. Its application to the process chain has been described in [7].

Flight Mission simulation

Typically, the use case for an engine is a Request for proposal (RFP) of a fixed aircraft with detailed requirements for engine weight and efficiency. The calculated engine designs in this study differ significantly in weight and efficiency, an adaption to a fixed aircraft would lead to different aircraft operating distances or to a change in aircraft payload. These influences are difficult to balance, therefore such a fixed use-case is not applicable here.

Instead, a fixed transport task is defined, and a fixed aircraft base technology is assumed. The aircraft characteristic is then iteratively adapted to the engine design as shown in Figure 8. This flight mission analysis poses a possibility to define a suitable figure of merit for both considered engine concepts and all different engine designs.

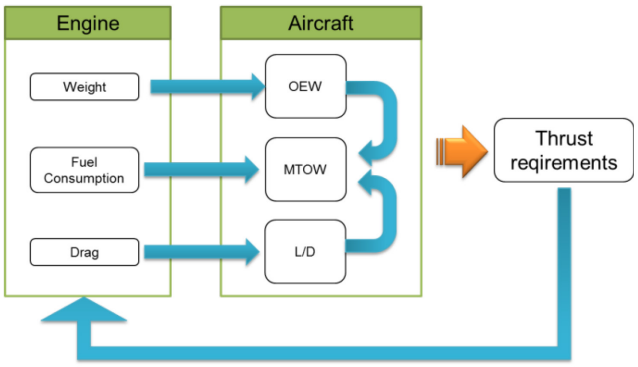

Figure 8: Schematics of the interaction between aircraft and engine in the design process

A future wide body airplane is selected as baseline configuration. Its key technology parameters are taken from an early design estimation of the Boeing 787 [22] as described in [7].

The mission calculation is performed backwards. The descend segment is neglected as it has a very small effect on fuel burn for a long range mission. The Breguet equation (Eq. 3)

$$R = \frac{v_{Flight}\left(\overline{L/D}\right)_{corr}}{g*\overline{TSFC}} * \ln\frac{m_{Cruise,init}}{m_L} \qquad (3)$$

is applied to calculate the weight at initial cruise $m_{cruise,init}$ for a given mission length R.

The landing weight (m_L) depends on the operating empty weight, the payload and the reserve fuel (Eq. 4):

$$m_L = \text{OEW+Payload+ReserveFuel} \qquad (4)$$

A constant payload is assumed. The OEW includes the engine and nacelle weight [7]. The lift-to-drag ratio $\left(\overline{L/D}\right)_{corr}$ is calculated for each engine design and includes the engine relate drag [7].

After deriving the average specific fuel burn $\overline{TSFC}$ from the performance simulation, the aircraft weight at initial cruise can be derived leading to the required thrust at cruise. The thrust at Top of Climb is calculated for a given rate of climb.

Based on engine performance calculations, an averaged climb fuel flow is determined for a fixed climb segment duration of 28 minutes to calculate the maximum takeoff-weight (MTOW).

The EoF thrust requirement is calculated at zero altitude for a flight Mach number of 0.25 using MTOW. As in this condition flap and landing gear are deployed, an adapted L/D of 16.58 and a climb angle of 8.2° (according to [16]) are assumed in order to calculate the EoF thrust.

With this approach, the thrust requirements for the engine cycle are defined iteratively as they depend on the engine weight and appropriate dimensions. The engine size influences the drag and thus reduces L/D, while the engine weight affects aircraft OEW.

The assumptions on aircraft and mission performance are summarized in Table 2.

L/D @ Cruise	-	20.84
L/D @ EoF	-	16.58
Rate of Climb @ TOC	*ft/min*	640
ClimbAngle @ EoF	°	8.2
Reference Area	m^2	359.5
OEW	*kg*	108501
Payload	*kg*	21337 (224Pax)
Mission Length	*nm*	8400
Holding Time	*min*	30
Dst. To Alternate	*nm*	200
Ref. Engine weight	*kg*	5048
Ref. Nacelle weight	*kg*	1951

Table 2: Aircraft assumptions, from [22]

3.2 Results

The aerodynamic design (chapter 2) has created various response surfaces that represent the Pareto-fronts for optimized fan efficiencies and weights.

These response surfaces return i.e. the fan isentropic efficiencies or the rotational design speeds as functions of axial fan inlet Mach number ($Ma_{ax,fan}$) and unscaled fan weight for each regarded fan pressure ratio.

In a first step, the best compromise between (unscaled) fan weight and efficiency is derived for discrete Π_{fan} and $Ma_{ax,fan}$ in order to reduce the design space. Herefore, the beforementioned mission based cycle design methodology is applied to multiple points on each Pareto front. Thus, for each fan design, the corresponding engine cycle and the required mission fuel burn is derived.

The exemplary results for the CR-fan at Π_{fan}=1.3 are shown in Figure 9, the corresponding results for the SR-fan are presented in Figure 10.

For all $Ma_{ax,fan}$ <0.7, the best compromise between fan weight and fan efficiency in terms of mission fuel burn can be found within the Pareto-front. For higher values of $Ma_{ax,fan}$, the minimal fuel burn was found at the highest unscaled fan weights.

The CR-fan data shows discontinuities for the low values of $Ma_{ax,fan}$ that stem from changes in the number of compressor stages. The stage number of the compressors and turbines is derived assuming a maximal stage loading and is affected by the selection of the fan pressure ratio, and its efficiency. Especially the number of LPT stages increases towards low fan pressure ratios, resulting in higher engine weights.

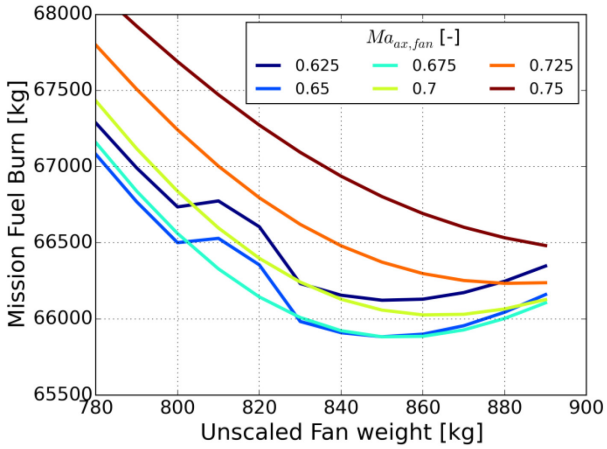

Figure 9: Mission Fuel burn for CR-fan engines for $\Pi_{fan} = 1.30$ as a function of the unscaled fan weight and $Ma_{ax,fan}$

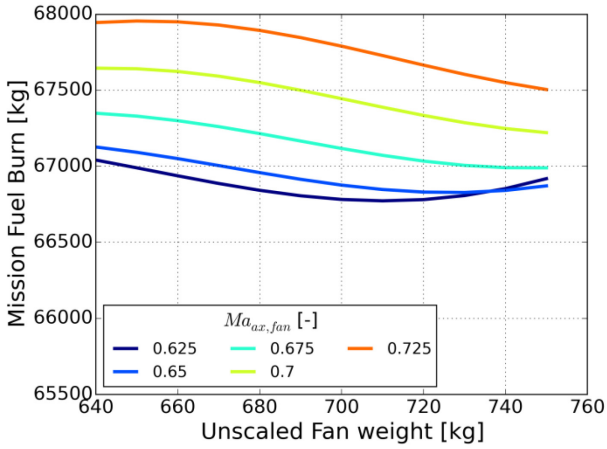

Figure 10: Mission Fuel burn for SR-fan engines for $\Pi_{fan} = 1.30$ as a function of the unscaled fan weight and $Ma_{ax,fan}$

For the further study, only the minimum fuel burn of each curve is considered, eliminating the unscaled fan weight from the parameter range.

The propulsive efficiency of both concepts is mainly driven by the fan pressure ratio (Figure 11). It shows only minimal difference between the CR- and the SR-fan.

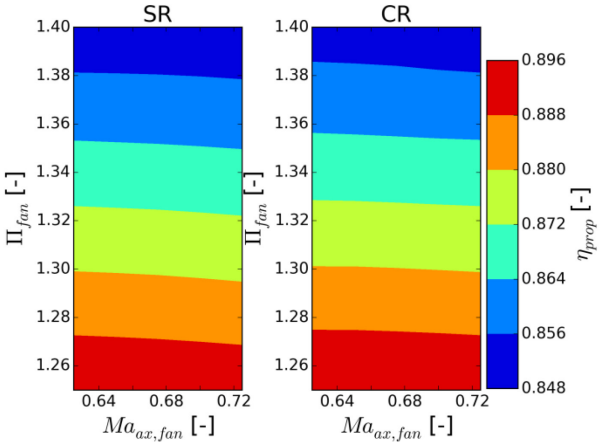

Figure 11 Propulsive efficiency η_{prop}

The thrust specific fuel consumption is shown in Figure 12. The CR-fan offers lower specific fuel consumption especially at high values of $Ma_{ax,fan}$. The reason is found in the higher isentropic efficiency of the CR-fan and in its comparatively low efficiency drop towards high axial Mach numbers.

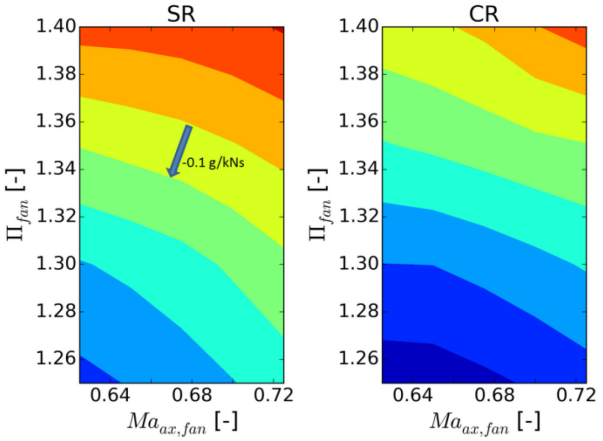

Figure 12: Engine TSFC for CR- and SR-fan engines at same scale. One colorstep= +-0.1 g/kNs

In Figure 13 the resulting engine weights are compared. The low fan pressure ratios require large and therefore heavy engines resulting in higher thrust requirements that increases engine weight even further. The CR-fan is heavier than the SR-fan, especially at low Π_{fan} due to the higher diameters and therefore higher relative weight share of the fan

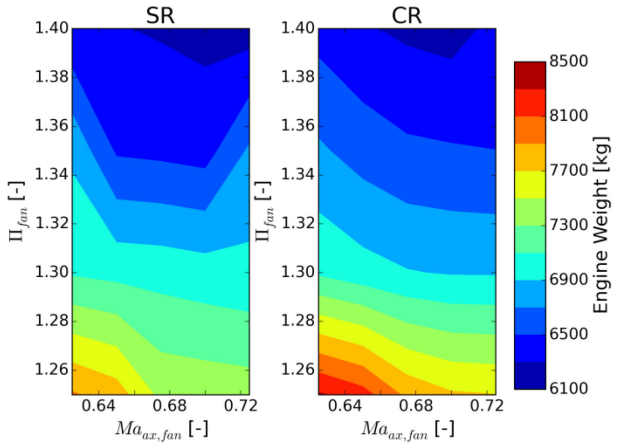

Figure 13 Calculated engine weights for SR-fan and CR-fan engines

To assess the effects of engine weight, drag and efficiency the mission fuel burn is used. For the CR-fan, the optimum fuel burn is derived as a function of Π_{fan} and $Ma_{ax,fan}$ in Figure 14. It shows an overall minimum at a Π_{fan} of about 1.3 and an $Ma_{ax,fan}$ of 0.65-0.69. These results are similar to previous results ([7]) for CR-fans without optimized weights.

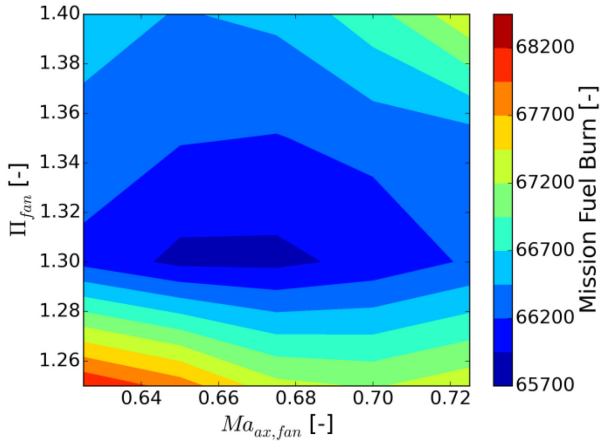

Figure 14: Mission Fuel Burn of CR-fan engine

The corresponding results for the SR-fan engines are presented in Figure 15. Here the optimum fuel burn is found at higher Π_{fan} of about 1.35 while the ideal $Ma_{ax,fan}$ is slightly lower than for the CR-fan engines.

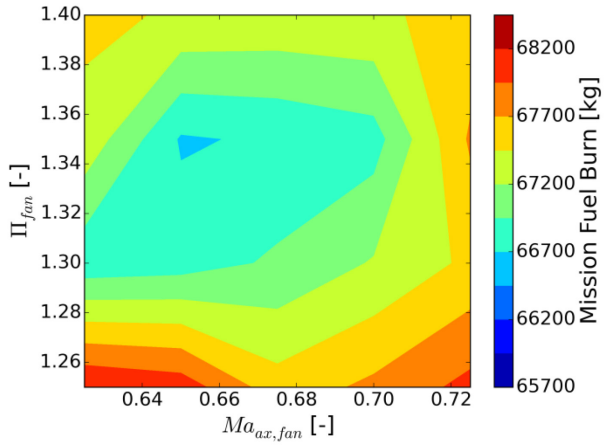

Figure 15: Mission Fuel Burn of SR-fan engines

The relative difference of both engine concepts is shown in Figure 16. The highest benefit of the CR-fan engines is found at high $Ma_{ax,fan}$ and $1.3<\Pi_{fan}<1.35$. The maximum fuel burn reduction of the CR-fan engines at this point is 2.1%. At other conditions, the difference between both concepts is smaller. In the region of the fuel burn optima, the difference is about 1%.

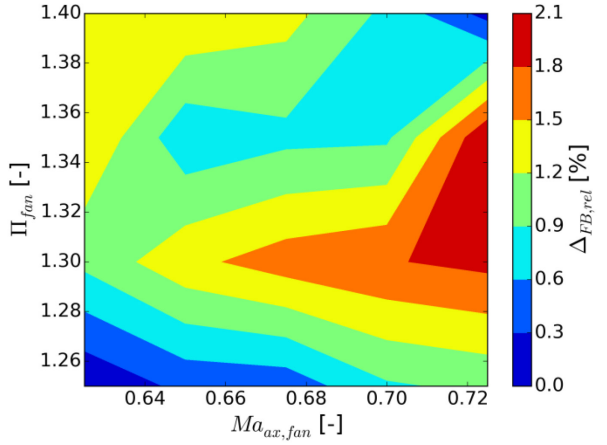

Figure 16: Relative Mission Fuel Burn difference $\Delta_{FB,rel} = \frac{FB_{SR}-FB_{CR}}{FB_{SR}}$

3 Summary and Outlook

An optimization approach for the design of different fan concepts is presented and applied to counter- and single-rotating fans in order to optimize its aerodynamic efficiency and its weight for various fan pressure ratios and axial

Mach numbers. The optimization process chain consists of a CFD simulation and a structural analysis of the blades. As a result of this optimization a function of the maximal achievable efficiency vs. minimal fan module weight are derived.
These results are directly transferred to an engine performance study coupled with a flight mission analysis. This approach allows a simple integrated assessment of the effects of various propulsors on cycle design and integration effects.

The ideal fan pressure ratios and axial fan inlet Mach numbers for both fan concepts are derived for given technology assumptions by comparing the fan designs on a given flight mission.

The results show a small mission fuel burn benefit for the counter rotating fan that increases with axial fan inlet Mach numbers to a maximum of 2%. This is due to the higher aerodynamic efficiency in this area.

The best mission fuel burn was found for a fan pressure ratio of ~1.3 for the CR, and ~1.35 for the SR-fan. The best axial Mach numbers hardly differ between the CR-fan (0.67) and the SR-fan (0.66). The mission fuel burn difference between the best CR- and SR-fan is ~1.4%.

The weight disadvantage of the CR-fan becomes dominant at very low fan pressure ratios, minimizing its fuel burn benefit in this region.

Summing up the results of this study, it remains questionable, if the comparatively low benefit of the CR-fan justifies the development of a corresponding engine. However, the increasing efficiency benefit towards high axial Mach numbers indicates, that the CR-fan might pose a good option for a use-case with much higher importance of the engine size. The lower ideal fan pressure ratio might pose advantages for the noise reduction despite the potentially more complex low noise design due to the interaction of the blade rows [27].

In a next step, a direct coupling of the engine performance software GTlab-Performance and the aerodynamic and mechanical predesign and design tools will further enhance the flexibility of the analysis.

Furthermore, the engine conceptual design tool GTlab-Sketchpad [25] is currently in development at DLR and will improve the reliability of the geometry and weight assessments.

References

[1] Otten, T.; Lengyel-Kampmann, T.; Nicke, E.; *Influence of a Planetary Differential Gear on Counter Rotating Fan Performance*, 49th AIAA/ASME/SAE/ASEE Joint Propulsion Conference, San Jose, California, USA, 2013

[2] Talbotec, J.; Vernet, M.; *SNECMA Counter Rotating Turbo Fan Aerodynamic Design Logic & Tests Results*, ICAS 2010-4.1.2

[3] Khaletskiy, Y.; Mileshin, V.; Talbotec, J.; Nicke, E.; *Study on noise of counter rotating fan models at CIAM anechoic chamber*, ICAS 2012

[4] Lengyel-Kampmann, T.; Nicke, E.; Rüd, K-P.; Schaber, R.; *Optimization and Examination of a Counter Rotating Fan Stage – The possible Improvement of the Efficiency Compared with a Single Rotating Fan.* 20th ISABE Conference, Göteborg, Sweden, ISABE-2011-1232, 2011

[5] Lengyel-Kampmann, T.; Voss, C.; Nicke, E; Rüd, K-P.; Schaber, R.; *Generalized optimization of counter-rotating and single-rotating fans*, ASME Turbo Expo Conference, Düsseldorf, Germany, ASME-GT2014-26008, 2014

[6] Lengyel-Kampmann, T.; Otten, T.; Schmidt, T.; Nicke, E.; *Optimization of an engine with a gear driven counter rotating fan PART I: Fan performance and design. 22th ISABE Conference,* Phoenix, Arizona, USA, ISABE-2015-20091, 2015

[7] Otten, T.; Lengyel-Kampmann, T.; Becker, R.; Reitenbach, S.; *Optimization of an Engine with a gear driven counter rotating fan PART II: Cycle selection and Performance*; ISABE, *22th ISABE Conference,* Phoenix, Arizona, USA ISABE-2015-20090, 2015

[8] Nürnberger, D.; Ashcroft, G.; Schnell, R.; Kügeler, E.; *Turbomachinery Research Aerodynamics Computational Environment (TRACE) User´s Manual*, 2006

[9] Dhondt, G.; *http://www.calculix.de/*

[10] Voß, C.; Aulich, M.; Kaplan, B.; Nicke, E; *Automated Multi-objective Optimisation in Axial Compressor Blade Design*, ASME Turbo Expo, GT2006-90420

[11] Siller, U.; Voß, C.; Nicke, E.; *Automated Multidisciplinary Optimization of a Transonic Axial Compressor*, AIAA Conference, AIAA-2009-0863

[12] Schmitz, A.; *Entwicklung eines objektorientierten und parallelisierten Gradient Enhanced Kriging Ersatzmodells*, DLR, FU Hagen, Masterarbeit, Köln, 2013

[13] Grieb, H.; *Projektierung von Turboflugtriebwerken*, Birkhauser Verlag, 2004
[14] Kurzke, J.; *Aeroengine Design: From State of the art turbofans towards innovative architectures*, VKI Lecture Series; von Karman Institute for Fluid Dynamics, 2013
[15] Kappler, G.R.; Staudacher, S.; *Gewichtsstudie zu Niederdrucksystemen moderner Turbofan-Triebwerke* DGLR, Deutscher Luft- und Raumfahrtkongress, 2012
[16] Sagerser, D.A.; Lieblein, S; Krebs, P.; *Empirical expressions for estimating length and weight of axial-flow components of VTOL powerplants,* 1971
[17] Jackson, A. J. B.; *Optimisation of aero and industrial gas turbine design for the environment*, Cranfield University, PhD Thesis, 2009
[18] Gunston, B. (Ed.); *Jane's Aero-Engines, Issue 12*, Jane's Information Group Ltd., Surrey, 2002
[19] Reitenbach, S.; Rittel, T. ; *Abschaetzung von Gewicht und Widerstand bei der Triebwerksvorauslegung*; DLR, Projektarbeit, 2011, Interner Bericht, IB-Nr. 325-09-15
[20] Hendricks, E.; Ton, M.: *Performance and Weight Estimates for an Advanced Open Rotor Engine*, NASA/TM—2012-217710
[21] Raymer, D.P.; *Aircraft Design: A Conceptual Approach*, Second Edition, ISBN 0-930403-51-7, 1992
[22] PIANO Website; http://www.lissys.demon.co.uk/samp1/ ; accessed 29.4.2015
[23] Tong, M.T.; *An Assessment of the Impact of Emerging High-Temperature Materials on Engine Cycle Performance*, ASME Turbo Expo 2010, GT2010-22361, 2010
[24] Larsson, L.; Kyprianidis, K.; Groenstedt, T.; *Conceptual Design and Mission Analysis for a Geared Turbofan and an Open Rotor Configuration*, ASME Turbo Expo 2011, GT2011-46451
[25] Becker, R.-G.; Reitenbach, S.; Klein, C.; Otten, T.; Nauroz, M.; Siggel, M.; *An Integrated Method for Propulsion System Conceptual Design*, ASME Turbo Expo 2015, GT2015-43251
[26] Kurzke, J. ; *How to get component maps for aircraft gas turbine performance calculations* ASME 1996, ASME 96-GT-16
[27] Moreau, A.; Guérin, S.; *The Impact of Low-Speed Fan Design on Noise: An Exploratory Study*, Journal of Turbomachinery Vol. 138, August 2016, ASME

8 Contact Author Email Address

tom.otten@dlr.de

Copyright Statement